Available online at www.sciencedirect.com
ScienceDirect
International Journal of Mass Spectrometry 263 (2007) 22–29
International Journal of Mass Spectrometry
www.elsevier.com/locate/ijms

Cello-, malto- and xylooligosaccharide fragmentation by collision-induced dissociation using QIT and FT-ICR mass spectrometry: A systematic study

Salla Pasanen, Janne Jänis, Pirjo Vainiotalo *

Department of Chemistry, University of Joensuu, P.O. Box 111, FI-80101 Joensuu, Finland

Received 17 October 2006; received in revised form 8 December 2006; accepted 8 December 2006
Available online 16 January 2007

Abstract

In order to study the effects of the precursor ion type and the carbohydrate structure on the fragmentation of neutral unsubstituted oligosaccharides in collision-induced dissociation (CID), a systematic study of deprotonated, protonated, ammoniated and alkali metal cationized cello-, malto- and xylooligosaccharides was carried out using a quadrupole ion trap (QIT) and Fourier transform ion cyclotron resonance (FT-ICR) mass spectrometry. The fragmentation pathway was highly dependent on the choice of the precursor ion type. Deprotonated precursors gave rise to both glycosidic and cross-ring fragmentation, with clear differences among the three oligosaccharides, therefore being the most prominent for structural analysis. The fragmentation behavior of the xylooligosaccharides differed from that of the cello- and maltooligosaccharides for all the precursor ions studied, most remarkably with the deprotonated and ammoniated precursors. Stereochemical differentiation of cello- and maltooligosaccharides was possible with the use of deprotonated, lithiated and sodiated precursors. In general, as the size of the alkali metal cation increased the amount of structurally informative cross-ring fragmentation increased, but the probability for metal ion loss from the precursor ion also increased. The CID spectra of xylooligosaccharides measured with the QIT and FT-ICR were surprisingly similar.

Keywords: Cellooligosaccharides; Maltooligosaccharides; Xylooligosaccharides; Collision-induced dissociation

1. Introduction

Soft ionization methods like fast atom bombardment (FAB), matrix assisted laser desorption/ionization (MALDI) and electrospray ionization (ESI) in combination with tandem mass spectrometry can provide information about sequence, linkage type and even the anomeric configuration of oligosaccharides [1–5]. For instance, energy resolved collision-induced dissociation (CID) mass spectra were recently used for distinguishing isomeric cello-, malto- and isomaltooligosaccharides [3].

The fragmentation of cello- and maltooligosaccharides has been previously studied using several different precursor ions (both positive and negative), including deprotonated [4,6–11], protonated [9,12], lithiated [13,14], sodiated [9,12,15–20], potassiated [9,14] and cesiated [14] molecules, as well as chloride adducts [21]. Moreover, for maltooligosaccharides up to maltohexaose, a systematic MALDI Fourier transform ion cyclotron resonance (FT-ICR) study was performed, which covered all alkali metal adducts [22]. In contrast, the fragmentation of xylooligosaccharides has been studied significantly less. Reis et al. prepared a mixture of neutral and acidic xylooligosaccharides by partial acid hydrolysis from olive pulp and measured CID spectra in both positive and negative ionization modes for several ionic species [23–27]. In addition, Matamoros Fernández et al. and Quéméner et al. studied arabinoxylans and also presented CID spectra for some precursor ions of neutral xylooligosaccharides [28–30].

In this study, the fragmentation of several different precursor ions of neutral, underivatized cello-, malto- and xylooligosaccharides was examined by CID with the use of a quadrupole ion trap (QIT) and FT-ICR mass spectrometry. Cello- and maltooligosaccharides are both composed of 1,4-linked glucopyranose rings, but are distinguished by different anomeric configurations at their glycosidic linkages (i.e., β and α, respectively). Xylooligosaccharides are composed of 1,4-linked xylopyranose rings with the anomeric configuration of β, differ-

* Corresponding author. Fax: +358 13 2513360.
E-mail address: Pirjo.Vainiotalo@joensuu.fi (P. Vainiotalo).

1387-3806/$ – see front matter © 2006 Elsevier B.V. All rights reserved.
doi:10.1016/j.ijms.2006.12.002

ing from cellooligosaccharides by the lack of a CH_2OH group at the pyranose ring position C-5. The extent and the pathway of the fragmentation, depending on the choice of the precursor ion type (deprotonated, protonated, ammoniated or alkali metal cationized) as well as the oligosaccharide structure, were systematically studied. The possibility for stereochemical differentiation of β and α-linked oligosaccharides by CID was also examined.

2. Experimental section

2.1. Materials and sample preparation

β-D-Cellooligosaccharides, cellotriose (Glc_3), cellotetraose (Glc_4), cellopentaose (Glc_5) and cellohexaose (Glc_6), were obtained from the Seikagaku Corporation (Tokyo, Japan), and β-D-xylooligosaccharides, xylobiose (Xyl_2), xylotriose (Xyl_3), xylotetraose (Xyl_4), xylopentaose (Xyl_5) and xylohexaose (Xyl_6), from Megazyme International Ireland Ltd. Co. (Wicklow, Ireland). Cellobiose (Glc_2), α-D-Maltooligosaccharides, maltotriose (Mal_3), maltotetraose (Mal_4) and maltopentaose (Mal_5), ammonium acetate and rubidium chloride were purchased from Sigma–Aldrich (Steinheim, Germany), lithium chloride from Fluka (Buchs, Switzerland), cesium chloride from ICN Biomedicals Inc. (Irvine, CA), sodium acetate from Riedel-deHaën (Seelze, Germany) and potassium acetate from Merck (Darmstadt, Germany). HPLC grade water was purchased from Rathburn (Walkerburn, Scotland). All reagents were of the highest purity available and were used without further purification.

Stock solutions of all alkali metal salts and oligosaccharides were prepared by accurately weighing and dissolving them in water to a final concentration of 1–2 mM. Samples were prepared by diluting stock solutions in 10 mM ammonium acetate (pH 6.9). For positive-ion measurements, the oligosaccharide concentration was 10 μM, except 40 μM for FT-ICR, and the alkali metal salt (when added) was 100 μM. For negative-ion measurements, the oligosaccharide concentration was 50 μM.

2.2. ESI QIT mass spectrometry

A Bruker Esquire 3000 plus QIT mass spectrometer (Bruker Daltonik GmbH, Bremen, Germany) equipped with an ESI source was used. Sample solutions were directly infused into the ion source at a flow rate of 120 μL/h in the positive-ion mode and 200 μL/h in the negative-ion mode. N_2 (LC–MS-NGM 11 nitrogen generator; Bruker Daltonik) was used as a drying (3 L/min in the positive-ion mode and 5 L/min in the negative-ion mode, unless stated otherwise, 275 °C) and nebulizing gas (11 psi) and He (grade 5.6, AGA, Espoo, Finland) as the buffer/collision gas. The high vacuum varied in the range of 10^{-6} to 10^{-5} mbar. In the positive-ion mode measurements, the following voltages were used: capillary −3.5 kV, end plate offset −500 V, capillary exit 100 V, skimmer 40 V, octopole-1 4.0 V, octopole-2 1.9 V, lens-1 −5.0 V and lens-2 −60 V. In the negative-ion mode the polarities of voltages were switched and the values of capillary exit and octopole-1 were changed to −160 and −6.0 V, respectively. Ion charge control target was 20 000 at the positive-ion mode and 10 000 at the negative-ion mode, while the maximum allowed acquisition time was 50 ms. The value for the trap drive was 52. Each spectrum was an average of 8–10 spectra collected within 1 min, each of these containing 30 individual scans that were averaged before being sent from the instrument to the data system. Mass spectra were externally calibrated with an ES Tuning Mix (Hewlett Packard, Palo Alto, CA). In the CID, both the precursor ion isolation and the fragmentation widths were 4.0 *m/z*, the length of fragmentation pulse was 20 ms and the low mass cut-off was 27%. The fragmentation amplitudes of 0.7, 0.85, 1.0, 1.5 V, and additionally 0.2 V for protonated and ammoniated molecules, were used at the positive-ion mode and 0.2, 0.3, 0.4 and 0.7 V at the negative-ion mode. The instrument was controlled and the data were processed with the use of a Bruker Daltonics Compass 1.1 for Esquire/HCT. All numerical results presented have been calculated as an average from three or four measurements.

2.3. ESI FT-ICR mass spectrometry

A Bruker BioAPEX II FT-ICR mass spectrometer (Bruker Daltonics, Billerica, MA) was used. Ions were produced in an external Analytica of Branford (Branford, CT) ESI source. Sample solutions were directly infused, at a flow rate of 40 μL/h through a stainless steel capillary held at ground potential relative to the end-plate electrode at −3.7 kV. N_2 was used as a drying (10 psi, 200 °C) and nebulizing gas (15 psi). ESI-generated ions were transferred to the vacuum region of the instrument via a dielectric Pyrex capillary (entrance and exit potentials −4.2 kV and 210 V, respectively) prior to external accumulation in a radio frequency (RF) hexapole ($500V_{p-p}$ at 5.2 MHz) for 3.0 s. Ions were then extracted from the hexapole and focused/transferred to a cylindrical ICR cell (Infinity Cell) located inside a 4.7-T passively shielded superconducting magnet (Magnex Scientific, Abingdon, UK). Ions were captured inside the cell by a SideKick technique, excited to detectable cyclotron radii by an RF-sweep (72–480 kHz) and detected in a broadband mode. A total of 64 co-added 128-kword time-domain transients were recorded, zero-filled twice and finally subjected to fast Fourier transform and magnitude calculation. Mass spectra were externally calibrated using an ES Tuning Mix. For sustained off-resonance irradiation (SORI) CID, ions at a desired *m/z* were isolated by a correlated RF-sweep (2 ms, $\sim 36V_{p-p}$), followed by additional single-frequency excitation pulses (10 ms, $\sim 5V_{p-p}$) in order to eject any unwanted ions. The isolated ions were then excitated for 200 ms by a dipolar RF-field having a frequency (ν_{RF}) of 500 Hz below the ions' ICR frequency, and were allowed to collide with Ar (grade 4.8, AGA, Espoo, Finland) at $\sim 1.5 \times 10^{-6}$ mbar, introduced into the cell via a pulsed valve (General Valve, Fairfield, NJ). Within a 5-s pumpdown delay, the cell pressure rapidly fell to $\sim 5 \times 10^{-10}$ mbar prior to the detection event. The center-of-mass collision energy (E_{COM}) was calculated from the equation [32,33]:

$$E_{COM} = \left(\frac{m_n}{m_i + m_n}\right) \frac{q\beta^2 V_{p-p}^2}{8\pi B d^2} \frac{\nu_c}{\Delta\nu^2} \quad (1)$$

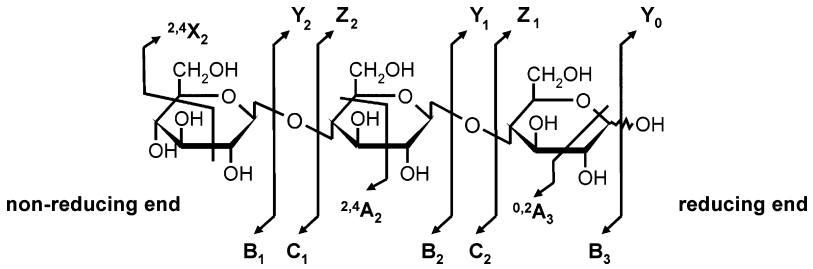

Fig. 1. Domon and Costello nomenclature [34] for oligosaccharide fragments illustrated for cellotriose.

where m_n is the mass of the collision gas, m_i the mass of the ion, q the charge of the ion, β the cell geometry factor (0.897 for Infinity Cell [31]), V_{p-p} the peak-to-peak excitation voltage of the RF-field, B the magnetic field strength, d the cell diameter (0.06 m), and ν_c is the reduced cyclotron frequency of the ion and $\Delta\nu = \nu_c - \nu_{RF}$ is the frequency offset of the RF-field. The instrument was controlled and the data were processed with the use of Bruker XMASS software, version 5.0.6.

2.4. Product ion assignment

Domon and Costello nomenclature for the oligosaccharide fragment ions was used (Fig. 1) [34]. However, since non-reducing and reducing end fragments cannot be distinguished (i.e., B from Z and C from Y) with the oligosaccharides studied, and additionally it is possible that for example $^{0,2}A_4$ fragment is the product of cross-ring cleavage at the reducing end combined with the loss of the non-reducing sugar ring, all cleavage assignments presented here are tentative and have not been rigorously verified. It has been shown earlier [10,21] (by labeling the anomeric position with ^{18}O) that the glycosidic bond of deprotonated precursors cleaves at the reducing side of glycosidic oxygen forming C fragments, from which B fragments can be formed by a consecutive loss of water. Glycosidic bonds of protonated [34,35] and metal cationized [21,36] precursors are instead predominantly cleaved at the non-reducing side, producing B and Y fragments. Due to the absence of a CH_2OH side chain at position C-5, $^{2,4}A$ and $^{0,3}A$ fragments of xylooligosaccharides (loss of 90 Da) have exactly the same mass and cannot be directly distinguished. In general, diagnostic fragments for 1,4-linkage are $^{0,2}A$, $^{2,4}A$ [37], and for deprotonated precursors also $^{0,2}A–H_2O$ [10]. Due to the fact that the $^{0,3}A$ fragments have always been at low abundance and expected to be formed by some second-order mechanism [37], the observed fragments for xylooligosaccharides are more probably $^{2,4}A$ fragments than $^{0,3}A$ fragments.

3. Results

3.1. ESI QIT mass spectrometry

The CID results obtained for various precursor ions of Glc_2, Glc_3, Glc_4, Glc_6, Mal_3, Mal_4, Xyl_2, Xyl_3, Xyl_4 and Xyl_6 were qualitatively similar to those observed for pentaoses, therefore the spectra are provided as Supplementary data.

3.1.1. Deprotonated precursors

Both deprotonated Glc_5 and Mal_5 mainly formed C fragments and only minor amounts of other fragments (Fig. 2(A) and (B), respectively), but a clear difference in the amount of A fragments was observed; Glc_5 also produced intense $^{0,2}A–H_2O$ fragments and the abundance ratio of $^{0,2}A–H_2O/^{0,2}A$ was almost four times greater for Glc_5 than for Mal_5 (7.0 ± 0.7 and 1.8 ± 0.3, respectively). In addition, the amount of $^{2,4}A$ fragments was smaller for Glc_5 than for Mal_5. The behavior of Xyl_5 (Fig. 2(C)) clearly differed from that of Glc_5 and Mal_5, most remarkably by the relative amount of glycosidic fragments (Table 1). In contrast to Glc_5 and Mal_5 the most abundant fragments for Xyl_5 were $^{0,2}A$ and $^{0,2}A–H_2O$, and $^{2,4}A$ fragments were completely absent. The intensity ratios of the C fragments were clearly different for all three oligosaccharides, as shown in Fig. 2.

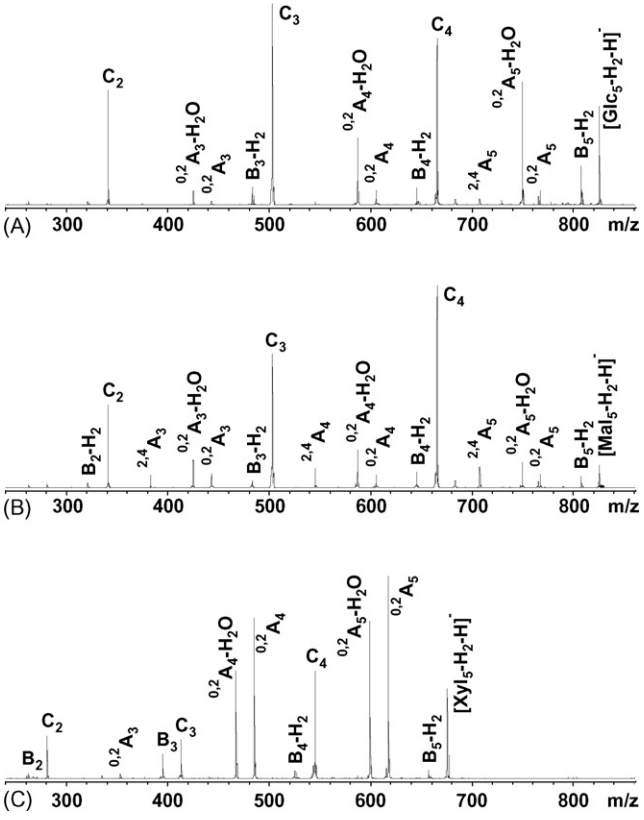

Fig. 2. CID spectra for deprotonated (A) cellopentaose, (B) maltopentaose, and (C) xylopentaose at a fragmentation amplitude of 0.4 V.

Table 1
Relative amounts (%) of observed fragments in CID for different precursors of cello-, malto- and xylopentaose

Fragment ions	Glc_5	Mal_5	Xyl_5
$[M-H]^-$[a]			
B	3.0 ± 0.3[b]	n.d.	5.2 ± 0.8
C	61 ± 3	67 ± 1	19 ± 2
$^{0,2}A$	4.4 ± 0.2	8.7 ± 1.0	41 ± 2
$^{0,2}A–H_2O$	30 ± 2	15.2 ± 0.4	35 ± 3
$^{2,4}A$	1.7 ± 0.3	9.3 ± 0.5	n.d.
Glycosidic	64 ± 3	67 ± 1	24 ± 2
Cross-ring	36 ± 3	33 ± 1	76 ± 2
$[M+Li]^+$[a]			
B	69 ± 2	42.4 ± 0.9	54.9 ± 0.5
$B–H_2O$	1.1 ± 0.5	1.1 ± 0.1	n.d
Y	9.5 ± 0.3	26.2 ± 0.5	29.0 ± 0.4
$^{0,2}A$	16 ± 1	26.8 ± 0.6	14.1 ± 0.3
$^{2,4}A$	4.5 ± 0.4	3.5 ± 0.2	2.0 ± 0.1
Glycosidic	80 ± 1	69.7 ± 0.4	83.8 ± 0.4
Cross-ring	20 ± 1	30.3 ± 0.4	16.2 ± 0.4
$[M+Na]^+$[a]			
B	45.7 ± 0.7	28.4 ± 0.6	38.5 ± 0.5
Y	9.8 ± 0.3	29.0 ± 0.4	18.5 ± 0.4
$^{0,2}A$	30.3 ± 0.9	32.4 ± 0.6	36.8 ± 0.5
$^{2,4}A$	14.3 ± 0.5	10.1 ± 0.5	6.2 ± 0.4
Glycosidic	55.5 ± 0.5	57 ± 1	57.0 ± 0.7
Cross-ring	44.5 ± 0.5	43 ± 1	43.0 ± 0.7
$[M+K]^+$[a]			
B	24 ± 3	8 ± 3	5 ± 3
Y	4 ± 2	8 ± 4	n.d
$^{0,1}A$	n.d.	n.d.	3.6 ± 0.3
$^{0,1}A–H_2O$	n.d.	n.d.	3 ± 2
$^{0,2}A$	18 ± 4	29 ± 8	5 ± 1
$^{0,3}A$	12 ± 1	n.d.	n.d.
$^{2,4}A$	42 ± 4	56 ± 10	84 ± 3
Glycosidic	28 ± 4	15 ± 2	5 ± 3
Cross-ring	72 ± 4	85 ± 2	95 ± 3

n.d., not detected at appreciable amounts (relative amount < 1%).
[a] Precursor ion.
[b] Relative amounts of individual fragments were obtained by dividing the intensity of the peak by the sum of the intensities of all fragments. Represented relative proportions ± S.D. were calculated as averages from four measurements, except for lithiated precursors, which were calculated from three measurements.

Interestingly, B fragments for all three oligosaccharides were mainly observed as B-2 fragments, corresponding to the elimination of H_2. The loss of H_2 directly from deprotonated precursors was also observed. The relative abundances of these fragments varied greatly from day to day, therefore $B–H_2$ fragments were discarded in all calculations (Table 1). If the elimination of H_2 from the precursor ion was not observed, $B–H_2$ fragments were absent too, and for Glc_5 and Xyl_5 minor B fragments were observed. Mal_5 did not form B fragments at all.

3.1.2. Protonated and ammoniated precursors

It is known that ammonium adducts of oligosaccharides are quite labile and that they readily lose NH_3 when forming protonated molecules [38]. Actually, an increase in the drying gas flow from 3 to 6–7 L/min was already enough to lose all ammoniated precursors. During the isolation of ammoniated precursors, protonated molecules were also observed at various abundances, except for Xyl_5 that did not form abundant protonated molecules under any conditions. Ammonium adducts behaved in the CID as expected, first forming protonated molecules with the loss of NH_3, which then dissociated further. Glc_5 and Mal_5 produced only B and Y fragments (Fig. 3(A) and (B), respectively and Table S-1). Their spectra were very much alike, but Glc_5 fragmented to a lesser extent. Instead, Xyl_5 gave rise to up to five consecutive losses of water from each B fragment, as shown in Fig. 3(C) and Table S-1. Direct loss of water from ammoniated precursor was also observed. The loss of water from Xyl_5 was clearly favorable, since it already formed $B–nH_2O$ (n = 1–5) at a low fragmentation amplitude (0.2 V) (Fig. S-6c). With the same amplitude, much less abundant glycosidic fragments were formed from Mal_5 with an abundant protonated molecule and for Glc_5 only an ammonium adduct and protonated molecule were observed (Fig. S-6a and b, respectively).

The CID spectra for protonated Glc_5 and Mal_5 were almost identical (results shown in Table S-1), except that, as with ammoniated precursors, the extent of fragmentation was smaller for

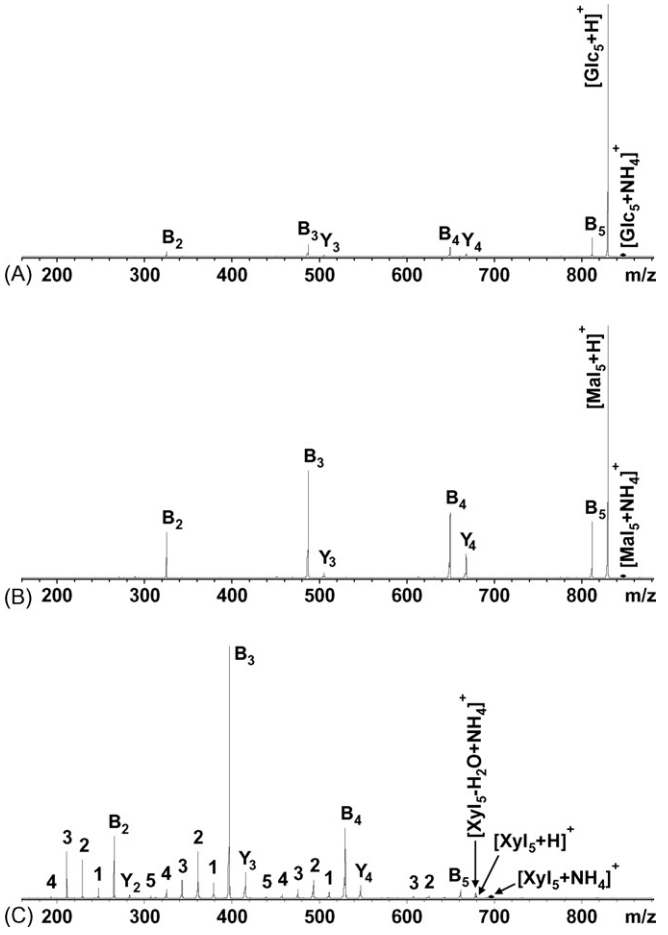

Fig. 3. CID spectra for ammoniated (A) cellopentaose, (B) maltopentaose, and (C) xylopentaose (peaks labeled by numbers represent $B–nH_2O$ ions, with the number corresponding to n) at a fragmentation amplitude of 1.0 V.

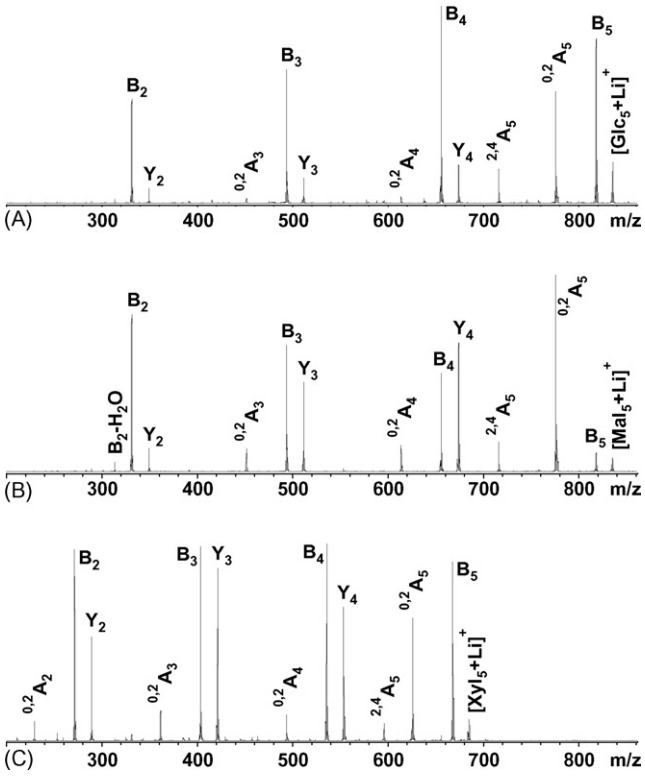

Fig. 4. CID spectra for lithiated (A) cellopentaose, (B) maltopentaose, and (C) xylopentaose at a fragmentation amplitude of 1.0 V.

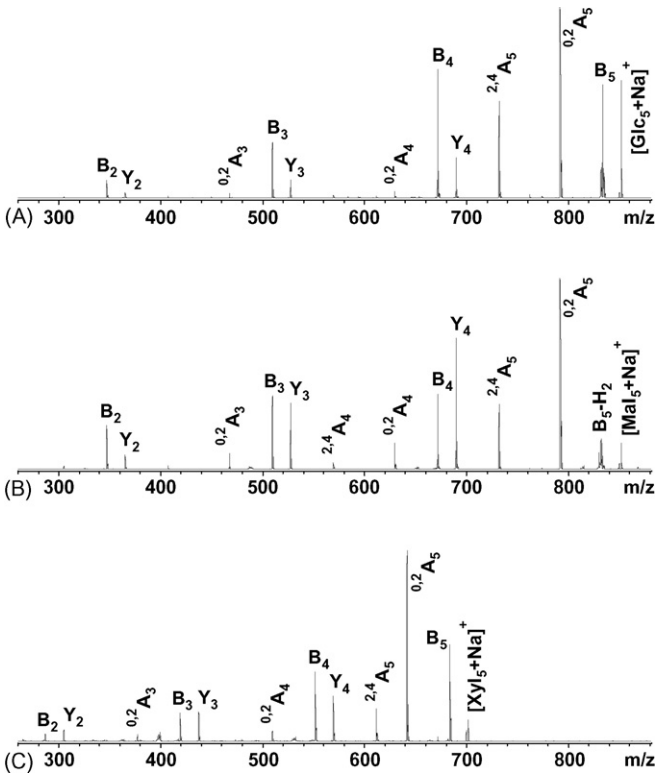

Fig. 5. CID spectra for sodiated (A) cellopentaose, (B) maltopentaose, and (C) xylopentaose at a fragmentation amplitude of 1.0 V.

Glc_5. Therefore, the source of the protonated precursor (obtained directly by increasing the drying gas flow rate up to 7 L/min or as a product from CID of the ammoniated precursor) had no observable effect on the CID spectra.

3.1.3. Alkali metal cationized precursors

As with previous observations made regarding maltooligosaccharides [22], abundant adducts for studied pentaoses were observed with all alkali metal cations, but larger alkali metal (rubidium and cesium) adducts dissociated via a metal ion loss without oligosaccharide fragmentation (data not presented). In general, the extent of fragmentation decreased with an increase in size of the alkali metal cation due to increasing tendency for metal ion loss, but the relative amount of cross-ring fragmentation increased (Table 1 and Figs. 4–6).

Even though the same fragments were formed, differentiation of Glc_5 and Mal_5 was possible since for both lithiated (Fig. 4(A) and (B), respectively) and sodiated precursors (Fig. 5(A) and (B), respectively) Y_4 and Y_3 fragments were clearly more abundant for Mal_5 than for Glc_5. The behavior of Xyl_5, however, differed from both Glc_5 and Mal_5, although the differences between the oligosaccharides were not that evident for sodiated precursors as for lithiated precursors; the abundance ratio of B_5 and $^{0,2}A_5$ fragments was similar with Glc_5 while the abundances of Y fragments were more likely similar with Mal_5 (Figs. 4 and 5). The behavior of the lithiated precursors was somewhat between protonated and sodiated precursors; cross-ring fragmentation was already observed but it was not as abundant as for the sodiated precursors (Table 1).

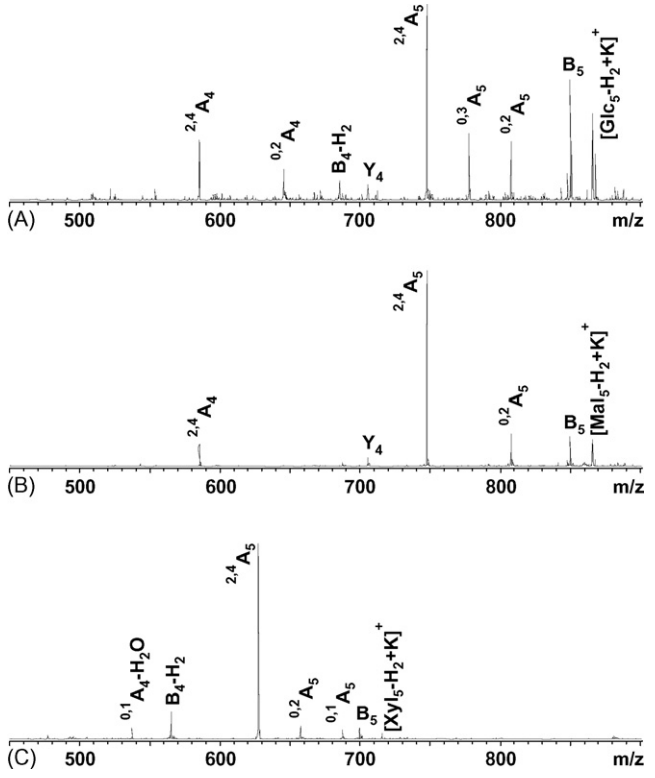

Fig. 6. CID spectra for potassiated (A) cellopentaose, (B) maltopentaose, and (C) xylopentaose at a fragmentation amplitude of 1.0 V.

Even though fragmentation was observed for the potassiated precursors, absolute intensities in the CID spectra were low due to the metal ion loss from the precursor ion. For Glc_5, $^{0,3}A_5$ and $^{0,2}A_4$ fragments were observed (Fig. 6(A)) but they were completely absent in the Mal_5 spectrum (Fig. 6(B)), and in addition, the B_5 fragment was more abundant for Glc_5 than for Mal_5. The $^{2,4}A$ fragments were clearly the most abundant fragments for all three oligosaccharides. Actually, for Mal_5 and Xyl_5 (Fig. 6(B) and (C), respectively) only minor amounts of other fragments were observed (even though the abundance of the $^{0,2}A_5$ fragment varied greatly for Mal_5), and the relative amount of cross-ring cleavages was greater than for the sodiated precursors. For Xyl_5, less abundant $^{0,1}A_5$ and $^{0,1}A_4$–H_2O fragments were also observed (Fig. 6(C)).

As with deprotonated precursors, the loss of H_2 from both the precursors and B_5 fragments were observed for sodium and potassium adducts for all three oligosaccharides but their relative abundance varied greatly from day to day, therefore these fragments were discarded in all calculations (Table 1).

3.2. ESI FT-ICR mass spectrometry

SORI-CID mass spectra for ammoniated and sodiated Xyl_5 (E_{COM} = 0.46 and 8.2 eV, respectively) are presented in Fig. 7 (the list of experimental and theoretical masses for the fragment ions are provided in Tables S-2 and S-3, respectively). The SORI-CID spectra were qualitatively similar in comparison to the corresponding CID spectra acquired with the QIT instrument (Figs. 3(C) and 5(C)). In addition to B and Y fragments, a characteristic pattern of sequential water losses (up to four) was evident for the ammoniated precursor, whereas the sodiated precursor fragmented mainly via glycosidic and cross-ring cleavages resulting in B, Y, $^{0,2}A$ and $^{2,4}A$ fragment ions. To gain information about the lowest energy dissociation pathways for both precursor ions, E_{COM} was stepwise increased from the values that did not induce any fragmentation to the threshold values at which the first fragments appeared. The lowest energy fragments were a protonated molecule for the ammoniated precursor by the corresponding loss of NH_3 and the cross-ring cleaved $^{0,2}A_5$ fragment for the sodiated precursor (spectra not presented), similarly as earlier reported for ammoniated N-linked oligosaccharides [38] and for sodiated Mal_4 [39]. The threshold value (E_{COM}) for fragmentation was found to be much lower for the ammoniated (~0.15 eV) than for the sodiated (~2.2 eV) Xyl_5. These results are in line with observations made from the QIT measurements and earlier reported results [40]. Interestingly, the ratio of glycosidic and cross-ring fragmentation for sodiated Xyl_5 (58:42) was almost identical to the ratio obtained with the QIT instrument (57:43), with the same extent of fragmentation. In addition, the intensity ratio of Y and Σ(B, B–nH_2O) fragments for the ammoniated precursors was similar in both the QIT and FT-ICR measurements (6:94 and 9:91, respectively), despite the different extent of fragmentation. These observations were quite surprising since more variation in the ion abundance due to the different techniques applied could be expected. The SORI-CID mass spectra for ammoniated and sodiated Xyl_4 were similar to those reported for Xyl_5 (data not presented).

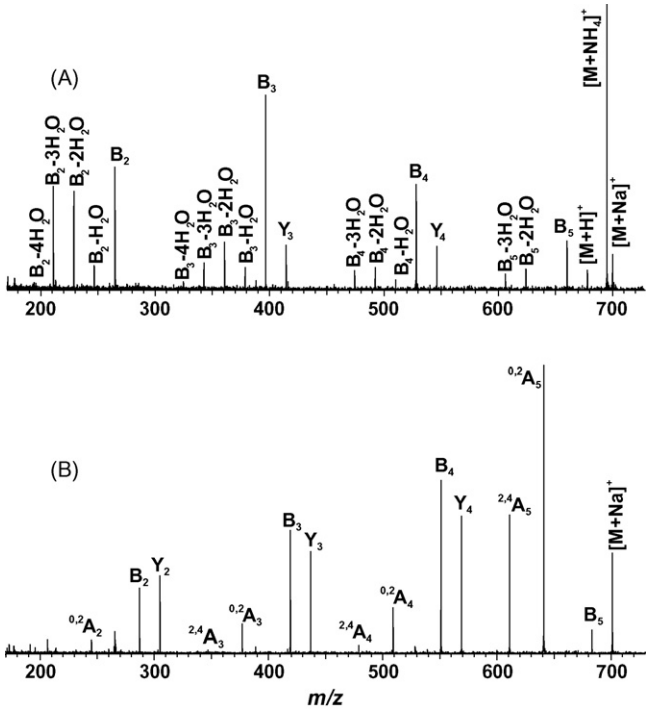

Fig. 7. SORI-CID mass spectra of (A) ammoniated and (B) sodiated xylopentaose with center-of-mass collision energies (E_{COM}) of 0.46 and 8.2 eV, respectively.

4. Discussion

The fragmentation pattern, and therefore the amount of structural information, obtained in the CID of oligosaccharides is greatly influenced by the choice of the precursor ion type. Protonated molecules produce mainly sequence related fragments by glycosidic bond cleavages, while deprotonated and metal cationized molecules also produce structurally more informative fragments by cross-ring cleavages [41]. Mechanisms for cross-ring cleavages for deprotonated [6] and alkali metal cationized [36,37] precursors are represented elsewhere in detail. It has been shown earlier [10] that deprotonation occurs selectively with the anomeric hydroxyl, since it is the most acidic hydroxyl in the structure. The fragmentation of glycosidic bonds occurs stepwise from the reducing end towards the non-reducing end, by forming at each stage a one unit shorter fragment ion with a similarly deprotonated anomeric hydroxyl group. After a negative charge is localized at the reducing end, the fragmentation of this ring occurs rapidly [10].

Deprotonated Glc_5 and Mal_5 can be differentiated based on the abundance ratio of $^{0,2}A$–H_2O/$^{0,2}A$, which was four times greater for Glc_5 than for Mal_5. Interestingly, a clear increase in the relative amount of $^{0,2}A$ fragments was observed for Xyl_5 when compared to Glc_5 and Mal_5 (Table 1). A qualitatively similar ESI quadrupole time-of-flight (Q-TOF) CID spectrum for deprotonated Xyl_5 was recently published, although no losses of H_2 were observed [30]. Abundant B–H_2 fragments of deprotonated 1,3-linked disaccharides, and also occasionally present

in the spectra of other compounds at minor abundances, have earlier been reported by Garozzo et al. [10], and some other groups have observed C–H_2 and Y–H_2 fragments [17,42]. To the best of our knowledge, comparable spectra for deprotonated Glc_5 and Mal_5 have not been published but Friedl et al. [21] have presented ESI-QIT spectra for a chloride adduct of Glc_5, which formed a deprotonated ion and fragmented further.

Usually, only glycosidic bond cleavages are observed for ammoniated and protonated precursors [2,35]. The glycosidic oxygens are the most basic in the structure, therefore protons are expected to be localized there. Protonation of glycosidic oxygen allows the electrons of ring oxygen to be delocalized, and thus induces glycosidic bond cleavage. The mechanism of glycosidic bond fragmentation is therefore charge-induced [22]. The fact that Mal_5 fragmented with lower amplitudes is consistent with earlier observations [3,43] that α-glycosidic bonds cleave more easily than β-glycosidic bonds. The different behavior of Xyl_5 was a very interesting observation. Up to five losses of water from B fragments were observed by QIT (Fig. 3(C)) and up to four by FT-ICR (Fig. 7(A)), therefore the loss of water even from the next sugar ring seems to be more favorable than glycosidic bond cleavage. ESI-Q-TOF CID spectra for ammoniated xylooligosaccharides have been published earlier [23], but a water loss pattern was not that evident. A proposed mechanism for sequential loss of water from Xyl_5 is represented in Fig. 8, where an aromatic ring structure is formed at the reducing end. Viseux et al. have earlier reported the formation of a similar aromatic structure through losses of permethylated glycosylalcohols from oligosaccharides [40]. This process is blocked in Glc_5 and Mal_5 that contain CH_2OH at position C-5, most probably due to different charge localization. The proposed mechanisms with putative ion structures for the loss of water from glucose have earlier been presented by Berman et al. [44] and Madhusudanan [45]. The exact mechanism have not been verified, but mechanism presented by Berman et al. [44] is in line with the mechanism presented here containing the formation of conjugated double bond system. In contrast, mechanism presented by Madhusudanan [45] is not likely, especially presented tricyclic structure formed by only six carbons and three oxygens. However, it remains unclear whether protonation and subsequent water loss from the CH_2OH group, leading to the isomeric structure with the B_5 fragment, would explain this behavior in the case of Glc_5 and Mal_5.

Both the ionic radii and the charge density of metal affects the ability to obtain simple, structurally specific data from oligosaccharides [46]. Only a limited number of sites exist where metal must "fit", and on the other hand, the metal-oligosaccharide complex has to be stable enough to allow cross-ring fragmentation to occur. Unlike protons, metal ions are able to coordinate with several oxygens simultaneously, thus decreasing the destabilization of the glycosidic bond. The coordination of the metal ion to the ring oxygen causes the localization of the oxygen electrons, therefore prohibiting the glycosidic bond cleavage and coordination of larger cations minimizes the destabilization of glycosidic linkages and the degree of charge-remote cross-ring fragmentation increases with an increase in cation size [22]. It is known that lithium and, to some extent, sodium are the best alkali metals for structural analyses of linear oligosaccharides, since precursors coordinating larger alkali metal cations primarily lose the metal cations during excitation [35]. The

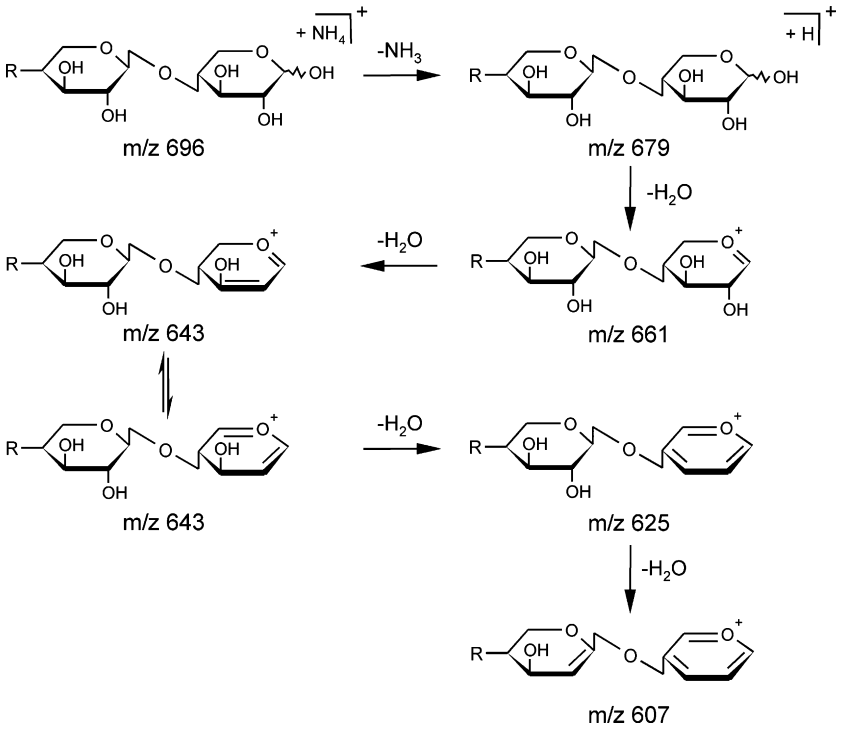

Fig. 8. Proposed mechanism for sequential loss of water from xylooligosaccharides illustrated for xylopentaose. Only the reducing end of the oligosaccharide is shown and the remaining sugar rings from non-reducing end are labeled as R.

same was observed in this study; even though the amount of structurally informative cross-ring fragments increased with an increase in the alkali metal cation size (Table 1), the fragmentation patterns of lithiated and sodiated precursors of all three oligosaccharides were characteristic to a certain precursor ion, but the reproducibility of fragmentation was clearly lower for potassiated precursors due to dissociation of potassium, and larger alkali metal adducts mainly dissociated. To the best of our knowledge, comparable spectra for lithiated and potassiated precursors have not been published. MALDI FT-ICR study for alkali metal adducts of Mal_2–Mal_6 have been presented [22] but the results were reported as percentage of a fragmentation, therefore comparison with these results cannot be made. Instead, sodiated precursors are widely studied and CID spectra for all three oligosaccharides can be found from the literature. Nanoelectrospray QIT CID spectra for sodiated Glc_5 and Mal_5 reported earlier by Bahr et al. [15] were qualitatively similar to our results, except that they observed only a negligible amount of ^{2,4}A fragments. The ESI-Q-TOF CID results for sodiated Xyl_5 published by Reis et al. [23,24] and Matamoros Fernández et al. [28] were slightly different. Reis et al. [24] observed mainly glycosidic cleavages (85%, calculated from relative abundances, compared to 57% obtained in this study) (Table 1 and S-3). The precursor ion was clearly less abundant in our study, indicating a greater amount of energy deposited to the precursor ion, therefore explaining the greater amount of cross-ring cleavages. Matamoros Fernández et al. [28] also observed more abundant glycosidic fragments, in comparison to our results.

Acknowledgements

Funding from The Graduate School of Bioorganic and Medicinal Chemistry in Finland and the Academy of Finland (Grant 108533) is gratefully acknowledged.

Appendix A. Supplementary data

Supplementary data associated with this article can be found, in the online version, at doi:10.1016/j.ijms.2006.12.002.

References

[1] D.M. Sheeley, V.N. Reinhold, Anal. Chem. 70 (1998) 3053.
[2] Z. Zhou, S. Ogden, J.A. Leary, Org. Chem. 55 (1990) 5444.
[3] A. Kurimoto, S. Daikoku, S. Mutsuga, O. Kanie, Anal. Chem. 78 (2006) 3461.
[4] B. Mulroney, J.C. Traeger, B.A. Stone, J. Mass Spectrom. 30 (1995) 1277.
[5] I. Fängmark, A. Jansson, B. Nilsson, Anal. Chem. 71 (1999) 1105.
[6] J.W. Dallinga, W. Heerma, Biol. Mass Spectrom. 20 (1991) 215.
[7] J.A. Carroll, L. Ngoka, C.G. Beggs, C.B. Lebrilla, Anal. Chem. 65 (1993) 1582.
[8] D.T. Li, G.R. Her, J. Mass Spectrom. 33 (1998) 644.
[9] C. Bosso, A. Heyraud, L. Patron, Org. Mass Spectrom. 26 (1991) 321.
[10] D. Garozzo, M. Giuffrida, G. Impallomeni, A. Ballistreri, G. Montaudo, Anal. Chem. 62 (1990) 279.
[11] A. Ballistreri, G. Montaudo, D. Garozzo, M. Giuffrida, G. Impallomeni, Rapid Commun. Mass Spectrom. 3 (1989) 302.
[12] R. Orlando, C.A. Bush, C. Fenselau, Biomed. Environ. Mass 19 (1990) 747.
[13] M.R. Asam, G.L. Glish, J. Am. Soc. Mass Spectrom. 8 (1997) 987.
[14] M.D. Mohr, K.O. Börnsen, H.M. Widmer, Rapid Commun. Mass Spectrom. 9 (1995) 809.
[15] U. Bahr, A. Pfenninger, M. Karas, B. Stahl, Anal. Chem. 69 (1997) 4530.
[16] A.S. Weiskopf, P. Vouros, D.J. Harvey, Rapid Commun. Mass Spectrom. 11 (1997) 1493.
[17] Y. Mechref, M.V. Novotny, C. Krishnan, Anal. Chem. 75 (2003) 4895.
[18] W. Tüting, R. Adden, P. Mischnick, Int. J. Mass Spectrom. 232 (2004) 107.
[19] A.H. Que, M.V. Novotny, Anal. Bioanal. Chem. 375 (2003) 599.
[20] C.S. Creaser, J.C. Reynolds, D.J. Harvey, Rapid Commun. Mass Spectrom. 16 (2002) 176.
[21] C.H. Friedl, G. Lochnit, R. Geyer, M. Karas, U. Bahr, Anal. Biochem. 284 (2000) 279.
[22] M.T. Cancilla, S.G. Penn, J.A. Carroll, C.B. Lebrilla, J. Am. Chem. Soc. 118 (1996) 6736.
[23] A. Reis, M.A. Coimbra, P. Domingues, A.J. Ferrer-Correia, M.R.M. Domingues, Rapid Commun. Mass Spectrom. 16 (2002) 2124.
[24] A. Reis, M.A. Coimbra, P. Domingues, A.J. Ferrer-Correia, M.R.M. Domingues, Carbohyd. Polym. 55 (2004) 401.
[25] A. Reis, M.R.M. Domingues, P. Domingues, A.J. Ferrer-Correia, M.A. Coimbra, Carbohyd. Res. 338 (2003) 1497.
[26] A. Reis, P. Pinto, M.A. Coimbra, D.V. Evtuguin, C.P. Neto, A.J. Ferrer-Correia, M.R.M. Domingues, J. Am. Soc. Mass Spectrom. 15 (2004) 43.
[27] A. Reis, P. Pinto, D.V. Evtuguin, C.P. Neto, P. Domingues, A.J. Ferrer-Correia, M.R.M. Domingues, Rapid Commun. Mass Spectrom. 19 (2005) 3589.
[28] L.E. Matamoros Fernández, N. Obel, H.V. Scheller, P. Roepstorff, Carbohyd. Res. 339 (2004) 655.
[29] L.E. Matamoros Fernández, N. Obel, H.V. Scheller, P. Roepstorff, J. Mass Spectrom. 38 (2003) 427.
[30] B. Quéméner, J.J. Ordaz-Ortiz, L. Saulnier, Carbohyd. Res. 341 (2006) 1834.
[31] H.L. Sievers, H.F. Grutzmacher, P. Caravatti, Int. J. Mass Spectrom. Ion Proc. 157/158 (1996) 233.
[32] J.W. Gauthier, T.R. Trautman, D.B. Jacobson, Anal. Chim. Acta 246 (1991) 211.
[33] Y. Huang, L. Paša-Tolić, S. Guan, A.G. Marshall, Anal. Chem. 66 (1994) 4385.
[34] B. Domon, C.E. Costello, Glycoconjugate J. 5 (1988) 397.
[35] L.C. Ngoka, J.-F. Gal, C.B. Lebrilla, Anal. Chem. 66 (1994) 692.
[36] G.E. Hofmeister, Z. Zhou, J.A. Leary, J. Am. Chem. Soc. 113 (1991) 5964.
[37] B. Spengler, J.W. Dolce, R.J. Cotter, Anal. Chem. 62 (1990) 1731.
[38] K.L. Duffin, J.K. Welply, E. Huang, J.D. Henion, Anal. Chem. 64 (1992) 1440.
[39] M.T. Cancilla, A.W. Wong, L.R. Voss, C.B. Lebrilla, Anal. Chem. 71 (1999) 3206.
[40] N. Viseux, E. de Hoffmann, B. Domon, Anal. Chem. 69 (1997) 3193.
[41] J.A. Carroll, D. Willard, C.B. Lebrilla, Anal. Chim. Acta 307 (1995) 431.
[42] L.P. Brüll, V. Kovácik, J.E. Thomas-Oates, W. Heerma, J. Haverkamp, Rapid Commun. Mass Spectrom. 12 (1998) 1520.
[43] T. Yamagaki, K. Fukui, K. Tachibana, Anal. Chem. 78 (2006) 1015.
[44] E.S.F. Berman, K.S. Kulp, M.G. Knize, L. Wu, E.J. Nelson, D.O. Nelson, K.J. Wu, Anal. Chem. 78 (2006) 6497.
[45] K.P. Madhusudanan, J. Mass Spectrom. 41 (2006) 1096.
[46] A. Fura, J.A. Leary, Anal. Chem. 65 (1993) 2805.